J. Ind. Geophys. Union, 28(6) (2024), 449-456

Fluid inclusion studies on mineralized and unmineralized granites of Malanjkhand Cu deposit in Central India

Deepa Arya
Department of Geology, Centre of Advanced Study, Kumaun University, Nainital- 263002, India
Corresponding author: arya.earth11@gmail.com

ABSTRACT

Our study presents fluid inclusion data on the mineralized and unmineralized granites from the Malanjkhand Cu deposit, Central India. Inclusions are recognized in quartz, which are similar in mineralized as well as unmineralized zones. These are monophase aqueous, biphase aqueous and polyphase (L+V+H) inclusions. The microthermometry results imply relatively high temperature (170-381.4 ^{0}C) of fluid entrapment in the mineralized granites, compared to considerably lower (169-235.8 ^{0}C) in unmineralized counterparts. Although, the salinity of fluid appears to be similar in both the variants, ranging from 4.07-15.47 wt% NaCl equivalent for mineralized granites and between 4.07 and 14.57 wt% NaCl equivalent for the unmineralized granites. The calculated salinity for mineralized granite (0.57-0.99 gm/cm^3) is found to be lower than the unmineralized granite (0.87-0.99 gm/cm^3). Textural and microthermometry results advocate that the hot brine fluid with lower density, generated from the mineralized granite silicic magma, was solely responsible for the ore deposition in mineralized veins and reefs, while cooler brine with high density fluid generated from unmineralized granite, was responsible for barren quartz veins.

Key words: Fluid inclusions, mineralized granite, unmineralized granite, Malanjkhand Cu deposit

INTRODUCTION

The hydrothermal deposits are one of the principal hosts of base metal deposits globally. The primary Cu ores are either porphyry or non-porphyry having close relationship with hydrothermal system. Globally, porphyry Cu deposits often produce Mo and Au along with Cu, and most of the major deposits are of Precambrian age (Richards and Mumin, 2013). Fluid inclusion studies of hydrothermal ore deposits have been recognized as an important tool to understand the thermodynamic environment of the hydrothermal fluids, responsible for the prevalent mineralization (Bean and Titley, 1981; Roedder, 1984). The fluid-inclusion characteristics such as fluid composition, temperature and density vary in different types of ore deposits; and to understand the variations in these parameters, fluid inclusions are considered a potential tool for mineral exploration (Haynes and Kesler, 1987; Noronha et al., 1992). Fluid evolution from host to hydrothermal system and ore mineral precipitation in hydrothermal systems, are recorded by multiple generations of fluid inclusion assemblages and mineral inclusions, and their trapping sequence can be established through detailed petrographic observations (Klemm et al., 2008; Seo et al., 2009).

The Paleoproterozoic Malanjkhand Cu deposit have been intensely investigated for a long time and much is known about the host-granite forming environment, age and tectonism (Sarkar et al., 1996; Panigrahi and Mookherjee, 1997; Sikka and Nehru, 1997; Stein et al., 2004; Asthana et al., 2016). however, the fluid inclusion studies on mineralized and unmineralized granite, are relatively fewer (Jaireth and Sharma, 1986; Panigrahi et al., 2008). The present study aims to test and document the potential of silicic magma responsible for vast and pervasive Cu deposit in the light of fluid inclusion petrography and microthermometry.

GEOLOGY

The Paleoproterozoic Malanjkhand pluton forms part of the Bastar Craton of central India. It is associated with three different lithological terranes such as Sausar Mobile Belt to the northwest which forms the southern part of the Central Indian Tectonic Zone (CITZ); the Sakoli Fold belt to the southwest; the Kotri-Dongargarh belt to the south. The Sausar Mobile Belt lies to the northwest part of Malanjkhand and marks the northern part of Central Indian Shear Zone (Figure 1a). The southernmost unit in the Satpura Mobile Belt is the Bhandara-Balaghat granulite domain bounded by the Central Indian Shear Zone to the south. Bastar craton (Bhandara) is composed of Archaean granites, granitoids, and mafic magmatic rocks, represented by mafic dyke swarms (Srivastava and Gautam, 2009; Srivastava et al., 2009; Chalapathi Rao et al., 2011) and is marked by presence of thickened continental crust since at least 3.6 Ga (Rajesh et al. 2009). The Bastar craton is unconformably overlain by supra-crustals and intracratonic Meso- to Neoproterozoic sedimentary sequences (Naqvi, 2005). The western part of peninsular India is covered by the vast and widespread volcanic complexes of Deccan Province (Pal and Bhargava, 1998; Bhowmik et al., 1999, 2000; Bhargava and Pal, 2000).

The geology of Malanjkhand pluton and associated litho-types including the mineralization aspects have been discussed in earlier studies (Tripathi, 1979; Rai and Venkatesh, 1993; Sikka and Nehru, 1997; Panigrahi and Mookherjee, 1997; Pal and Bhargava, 1998; Stein et al., 2004; Kumar et al., 2004a, b; Kumar and Rino, 2006, 2007). Malanjkhand pluton is basically an elongated N-S trending composite felsic bodies, emplaced at shallow-level, and covering an area of about 1500 sq km (Figure 1b).

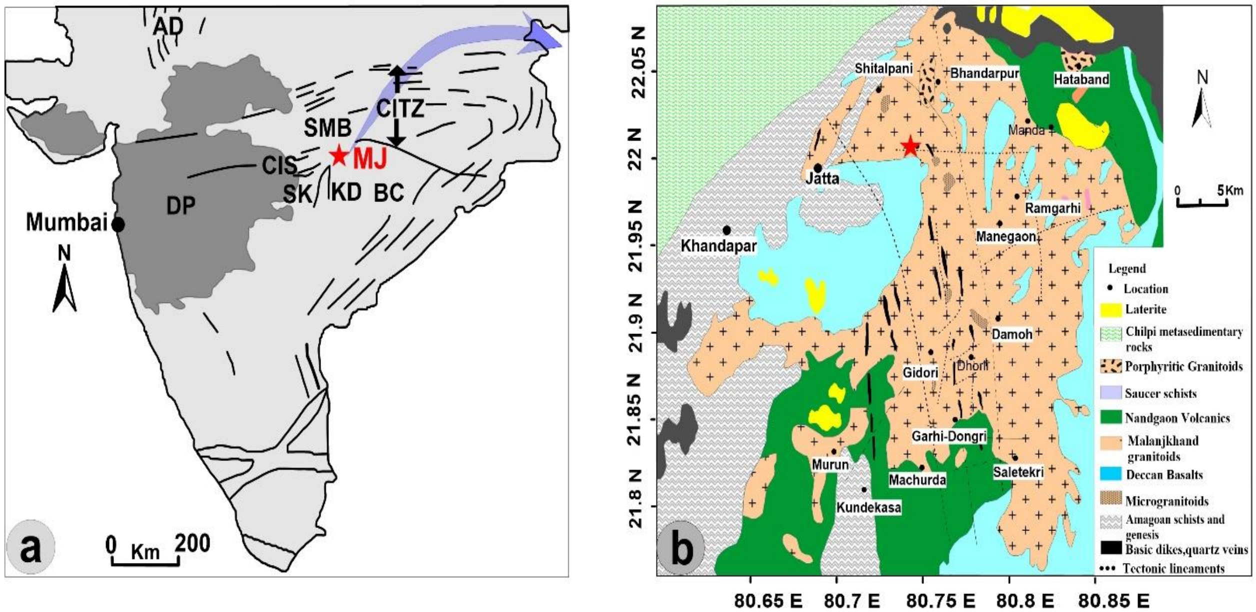

Figure1. (a) Generalized tectonic map of central and peninsular India (after Acharyya and Roy 2000; Stein et al. 2004). MJ refers to Malanjkhand which is our study area; AD: Aravalli Delhi Fold Belt, CITZ: Central Indian Tectonic Zone, SMB: Satpura Mobile Belt, CIS: Central Indian Shear, SK: Sakoli Fold Belt, KD: Kotri Dongargarh Belt, BC: Bastar Craton, DP: Deccan Province. **(b)** Geological map of Malanjkhand and surrounding area (after Bhargava and Pal, 2000; Kumar and Rino, 2006)

Table 1. Summarized microthermometry of type II fluid inclusions found in mineralized and unmineralized granites of Malanjkhand Cu deposit, central India.

Type of granite	Sample name	Temperature of first ice melting (^{0}C)	Temperature of final ice melting (^{0}C)	Temperature of homogenization (^{0}C)	Salinity (wt% NaCl equivalent)	Fluid density (gm/cm^3)
Mineralized granite	MG-1	-21.3 to -39.4	-2.5 to -11.5	171 to 381.1	4.07 to 15.47	0.57 to 0.99
	MG-2	-18.3 to -38.7	-4.3 to -21.1	170 to 261.8	6.37 to 15.07	0.84 to 0.99
Unmineralized granite	UG-1	-20.8 to -31.4	-3.3 to -14.5	169.2 to 212.7	5.62 to 14.46	0.92 to 0.99
	UG-2	-19.6 to -30.8	-2.3 to -10.6	175.8 to 235.8	4.07 to 14.57	0.87 to 0.98

The granitoids of Malanjkhand pluton are associated with the Nandgaon Group of volcano-sedimentary lithounits (Ramachandra and Rao, 1998), and are overlain by the Chilpi metasediments in the south-eastern and western parts of the pluton. Similarly, the older Amgaon schist and gneisses are exposed in the northwest and west of pluton, respectively. Nandgaon volcanics are exposed in the south and east of pluton. In the northeast of Malanjkhand pluton, the Deccan volcanics are exposed.

SAMPLE SELECTION AND METHODOLOGY

Representative samples of mineralized and unmineralized granites were collected from the Malanjkhand copper mine. A set of 4 samples comprising 2 each of mineralised (MG-1 and MG-2) and unmineralized (UG-1 and UG-2) granite samples, were selected on the basis of transparency and coarser grain size so that the inclusions can be easily seen.

The fluid inclusion studies have been carried at Fluid Inclusion Lab at Wadia Institute of Himalayan Geology (WIHG), Dehradun. For fluid inclusion analysis, doubly polished plates (0.05-0.1 mm thick) were prepared. For inclusion petrography, sample chips mounted on glass slides by canada balsam are used while for thermometric runs dismounted chips of <1 cm size (convenient to use in the heating-cooling chamber) are used. The doubly polished sections were studied by using optical microscopy and small chips (0.5 cm^2) containing fluid inclusions were broken off and mounted in the heating/freezing stage. Photographs were taken from each microscope field of view for the re-identification of individual inclusions. Fluid inclusions were also marked to relocate them for microthermometry which is performed using calibrated Linkam THMSG 600 fluid inclusion stage fitted on to Nikon E600 microscope. The acquired data is presented in **Table 1**, which is corrected within ± 0.2 ^{0}C at sub-ambient temperature and ±3 ^{0}C at total homogenization temperatures. Fluid inclusions were examined using a petrographic microscope to determine the size, shape, abundance, distribution and type of inclusions present in the rock samples. Individual inclusions were studied for their approximate size and the relative phase volumes using the spherical approximation (Roedder, 1984). Flicon computer program of Brown (1989) has been used for the fluid inclusion calculation.

PETROGRAPHY

Quartz within mineralized and unmineralized granites is significantly populated with fluid inclusions (Figures 2c, f). Different samples comprise more or less similar type, i.e., both mineralized and unmineralized granites consist Type-I, Type-II and Type-III inclusions (Figures 2 c, f.); however, they show a wide difference in the shape, size, position and abundance of the inclusions. Polyphase inclusions appear relatively fewer. Fluid inclusions in quartz are generally very small (2 µm), however, inclusions of bigger size (20 µm) have also been observed. These inclusions occur as isolated, in clusters or in trails, suggesting primary as well as the secondary origin. The overall population and size of fluid types in mineralized samples are small, ranging from 2 to 12 µm, except some large inclusions found in unmineralized sample having size of 12 to 20 µm. The primary inclusions in all associations are predominantly of aqueous biphase type, while the aqueous mono-phase inclusion appears secondary, since they exhibit cross cutting relationship with the grain boundary. On the basis of detailed petrographic studies, following types of inclusions have been observed in mineralised and unmineralized granitic samples.

Mineralised granites

Type I inclusions

These are monophase aqueous inclusions filled with aqueous solution at room temperature. The size of these inclusions is relatively small, ranging from 2 to 10 µm. These regular to semi-irregular in shape inclusions, occur as groups of 4 to 6 inclusions and as trails. The average population density of these inclusions is low (**Figure 2 a-c**). They sometimes appear to be coexisting together with bi-phase inclusions. They are transparent and have thin boundary.

Type II inclusions

These are bi-phase aqueous inclusions, consisting of liquid and a vapour phase at room temperature. These are the most common type of inclusions present in the mineralized granite sample. They are found as isolated and randomly distributed **(Figure 2 a-c).** However, some pseudo secondary trails of this type of inclusions are present. Shape of these inclusions varies from semi-rounded to irregular. Small elongated inclusions are also seen. Size of these inclusions vary from < 2 µm ~20 µm. Among the two phases, the liquid phase occupies ~80-90% and vapour phase about ~10-20% by volume respectively at room temperature. The gas bubble is aqueous vapour phase in composition. Some vapour bubbles are found in motion in small size inclusions, but are stationary in large size inclusions.

Type III inclusions

These are poly-phase or multiphase type of inclusions. They are present as isolated (Figure 2 c). Their size ranges from 5 to 6 µm and shape varies from regular to slightly tabular, however, larger one also seen with size up to 50 µm. In relatively bigger inclusions, the cubical halite and irregular sylvite crystal can also be observed easily (Figure 2 c).

Unmineralized granites

Type I inclusions

These are mono-phase aqueous inclusions occurring in trails. Their population density is moderate. They show cross cutting relationship with the grain boundary, to suggest secondary origin (Figure 2 e, f). Their size ranges from < 2 to 4 µm. They are regular to semi regular in shape, and coexist with biphase inclusions.

Type II inclusions

Bi-phase inclusions with aqueous liquid and vapour bubble are observed. The liquid-vapour proportion is 80-20% by volume. Their size ranges from 2 to 40 µm, which are large compared to bi-phase aqueous inclusions in mineralized granite (Figure 2 e, f). They are regular to semi irregular, equant to tabular in shape. They are randomly distributed throughout the sample. Trails of this type of inclusions are observed which are considered to be of secondary origin. The population density is moderately low. Vapour bubbles are found in motion in small inclusions and stationary in big size inclusions.

Type III inclusions

These are poly-phase inclusions, with liquid, vapour and solid phases (Figure 2 d, f). They are isolated and are relatively less abundant. Their size ranges from 4 to 8 µm, however, bigger size up to 30 µm have also been observed (Figure 2 d). In relatively bigger inclusions, the cubical halite and irregular sylvite crystal can be observed (Figure 2 d).

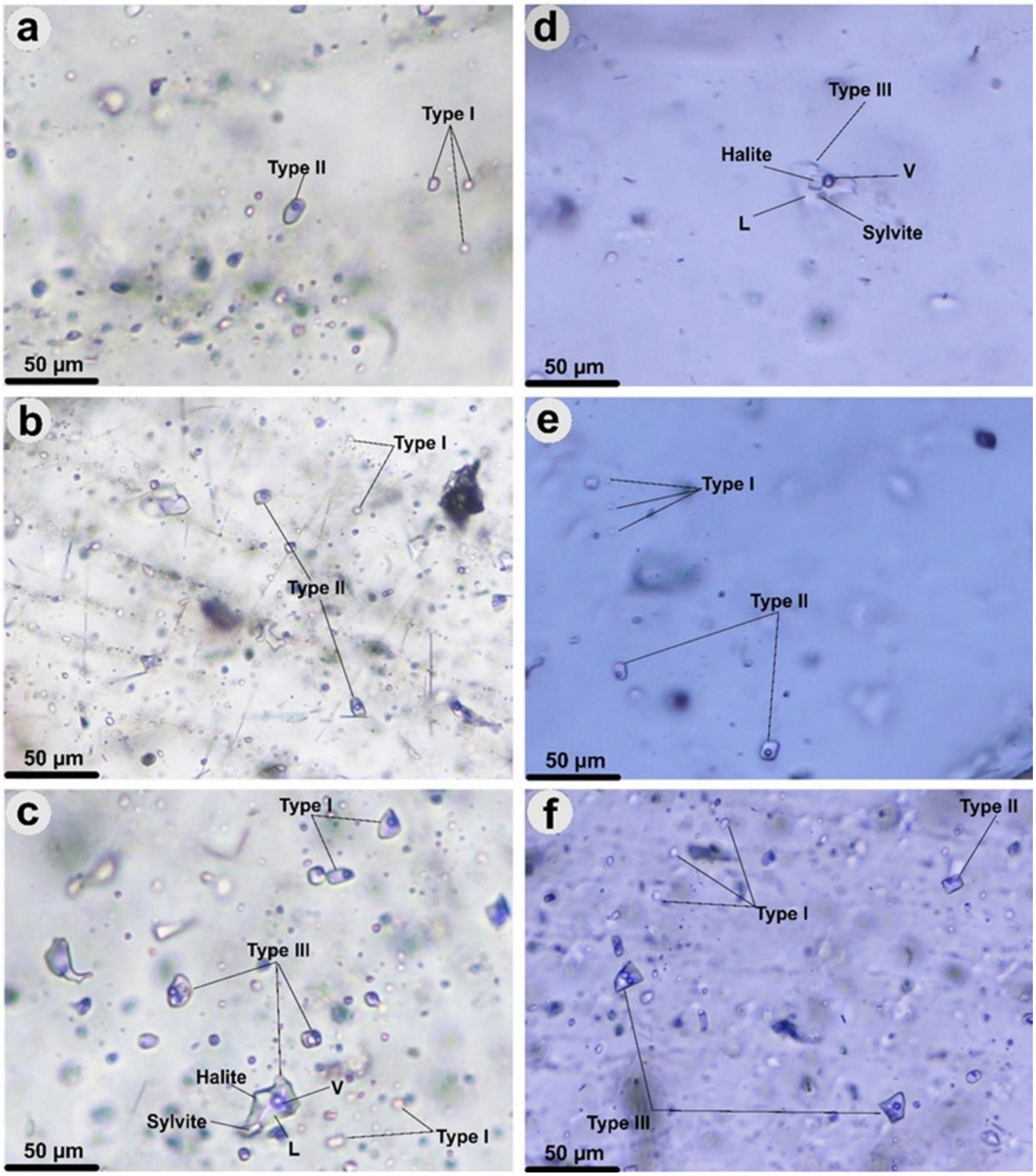

Figure 2. (a) Type I and II inclusions in mineralized granite. **(b)** Type I and II inclusions in mineralized granite. **(c)** Type I, II and III inclusions in mineralized granite. Presence of halite with cubical shape and sylvite with irregular shape in type III inclusion, **(d)** Type III inclusion in unmineralized granite. Presence of halite with cubical shape and sylvite with irregular shape. **(e)** Type I and II inclusion in unmineralized granite. **(f)** Type I, II, III inclusions in unmineralized granite

Table 2. Summary of heating-freezing characteristics of fluid inclusions in Malanjkhand Cu deposit in Central India.

Fluid inclusion type	Temperature range (^{0}C)	Observation	Interpretation
Type II Bi-phase inclusions	-40 to -80	Collapse of vapour bubble, shape become distorted.	Complete freezing of the fluid.
	-19 to -32	Inclusions becomes bright and bubble slightly becomes spherical.	First melting temp. or eutectic temperature.
	-2 to -10	Sudden movement of the vapour bubble and becomes perfectly spherical	Final melting temp. or freezing point temp.
	132 to 381	Disappearance of vapour bubble, completely one phase only.	Homogenization temp.

MICROTHERMOMETRY

The microthermometry of Type II inclusions in the mineralized and unmineralized granites have been performed. Table 2 presents the summary of heating-freezing characteristics of fluid inclusions in Malanjkhand Cu deposit. All inclusions are homogenised when they reaches the homogenization temperature suggesting that the fluid existed in one phase at the time of entrapment.

Heating-freezing experiments

The thermometric studies of the samples of Malanjkhand granitoid, reveal the composition, density and temperature conditions of the fluids during the mineral formation and migration. Microthermometry study confirms the evidence of but that much variation in inclusion types have not been observed. The phase changes on heating-cooling runs further confirm that aqueous fluids do exhibit temperatures and compositional variations. The results of microthermometric runs are shown in the Table 2.

Freezing studies

Freezing studies were carried out to determine the composition of inclusions from both mineralized and unmineralized granites. Inclusions were first frozen and phase changes were observed during gradual controlled warming. Heating rate close to the expected points of phase changes kept as low as 10 ^{0}C/min. Complete freezing of the inclusions was marked by the collapse of the vapour bubble with a sudden jerk and the shape become distorted. Attempts are made to check the metastability phase in mono-phase inclusions through cooling, but the inclusions does not show any nucleation of the bubble, and thus, they are not metastable fluid. It was also checked whether the dark appearing inclusions are hosting aqueous solution or filled with carbonic fluid. Microthermometric observation shows that these inclusions are made of simple aqueous solution. The first melting or eutectic temperature (T_{fm}) of the frozen inclusions occurred in temperature range of -18.3 ^{0}C to -39.4 ^{0}C. Accurate recording of the temperature of first melting temperature (eutectic temperature) is normally difficult and hence repeated freezing runs were undertaken to determine this temperature as accurately as possible. During the first melting temperature (T_{fm}) experiment, it was observed that the inclusion becomes dark and the bubble slightly attains the spherical shape. On further heating, the remaining ice crystal gradually melted, demarcating the final melting temperature (T_m) or freezing point temperature. In our study the final melting temperature range between -2.5 to -21.1^{0}C. The melting of the last ice crystal is recorded by sudden movement of the vapour bubble, and the bubble transforming into perfect spherical shape.

Heating studies

Selected fluid inclusions were heated in a temperature programmable heating-freezing system. Inclusions having irregular cavity boundaries or those showing signs of necking down were exempted. Heating was carried out at a constant rate of 10^0 C/min. The homogenization of biphase inclusion is clearly seen in a number of inclusions. During the gradual heating of the fluid, the vapour bubble progressively decreased in size and completely disappear when the fluids reached homogenization temperature. All inclusions of this study are homogenized in liquid phase thus any possibility of immiscible fluid phase/ boiling is ruled out. Their homogenization occurred at a wide temperature range of +169.2^{0}C to +381.1^{0}C. Though less in abundance, some inclusions from the mineralized granite samples are homogenized at above 300 ^{0}C also. The summary of the microthermometric observation and representative temperature of the significant change are given in Table 1.

Density

Density of the trapped fluid has been estimated using temperature of final ice melting (T_{fm}) and homogenization temperature (T_h) data in equation of Zhang and Frantz (1989). The density of the trapped fluids for mineralised and un-mineralized granitoids lie in the close range of 0.57-0.99 gm/cm^3 and 0.87-0.99 gm/cm^3 respectively. The variation of temperatures, salinity and density data in various samples is given in Table 1.

DISCUSSION

Obtained cryometric data for type II inclusions have revealed the variation in salinity of the trapped fluids. The final ice melting temperature in Type II inclusions present in quartz of mineralized granite, varies from -2.5 to -21.1 ^{0}C. Similarly, for unmineralized granites, it varies from -2.3 to -14.5 ^{0}C. Therefore, the ice-melting temperatures appear similar for both, with slightly higher for mineralized counterpart (Table 1). Likewise, the first ice melting temperatures in Type II inclusions are also in the similar range. The first ice melting temperature for mineralized granites varies from -18.3 to -39.4 ^{0}C and for unmineralized granites, from -19.6 to -31.4 ^{0}C. The observed first ice melting temperature for both the counter parts is close to the NaCl–KCl–H_2O eutectic, suggesting that very small amounts of $MgCl_2$/$CaCl_2$ may be present in NaCl–KCl–H_2O solution (Crawford, 1981; Roedder, 1984).

The homogenization data reveals significantly higher temperature of fluid entrapment in mineralized granite (170 to 381.1 ^{0}C) with respect to un-mineralized counterpart (169 to 235.8 ^{0}C) (**Table 1**). The studied type II inclusions homogenized by vapour disappearance. The estimates of the salinity of studied type II inclusions is based on their final ice-melting temperature and data of Hall et al. (1988) and Bodnar (1993). These values vary between 4.07 to 15.47 wt.% NaCl equivalent for mineralized granite and from 4.07 to 14.57 ^{0}C for unmineralizd granite. The salinity values for type II inclusions appear similar in variation for both types of granite (Table 1). The estimated density of type II fluid inclusions from mineralized granite is between 0.57 to 0.99 gm/cm^3 with higher frequency of low densities, although density of type II fluid inclusions from unmineralized granite appear to be significantly higher with low variation (0.87 to 0.99 gm/cm^3).

The monophase aqueous inclusions occur along with vapour inclusions, suggests boiling of fluid during entrapment (Mollai et al., 2009). Boiling is an effective ore depositional mechanism, and as the solution temperature decreases, the competence of metal deposition increases. Hence, as temperature decreases, the amount of dissolved metals in boiling hydrothermal solutions also decreases. Interestingly, results of petrography and microthermometry reveals boiling conditions during fluid entrapment in quartz crystals of mineralized as well as unmineralized granites, despite the fact that the low temperature of fluid entrapment in unmineralized granites.

Generation of hot brine fluid from the mineralized granite appear to be similar to that of mineralized veins at Malanjkhand Cu as proposed by Jaireth and Sharma (1986), therefore it would be prudent to say that increasing amounts of chlorine were partitioned into aqueous fluid exsolved from a crystallizing silicic magma of mineralized granite. Furthermore, cooler brine with higher density of late stage unmineralized granite supposed to have produced the barren quartz veins in the mine region. Nevertheless, high salinity seems to be common in both cases. This suggests no role of meteoric water during the fluid evolution. The relatively higher homogenisation temperature in mineralized granite inclusion, is significantly higher than in the unmineralized granite inclusion, which suggest that the high temperature saline fluid of lower density was responsible for ore deposition.

CONCLUSIONS

Following conclusions can be drawn from the present study:

(i) Mineralised granite was formed from H_2O- bearing hydrothermal solutions containing 4.07 to 15.47 wt% NaCl equivalent amount of chlorides of salt at temperature ranging from 171^{0}C to 381^{0}C.

(ii) A general predominance of NaCl-H_2O fluid is found in both mineralised as well as unmineralized granites.

(iii) Low temperature conditions (169^{0}C to 235 ^{0}C) prevail in unmineralized granite during the time of entrapment.

(iv) The salinity of the ore forming fluid is found between 4 and 15 wt% NaCl equivalent.

(v) The density of ore forming fluid ranged from 0.57 to 0.99 gm/cm^3.

ACKNOWLEDGEMENTS

Fieldwork and analysis are supported under a UGC grant (42-1008/2013/SR) and the Indian National Science Academy (INSA) Fellowship, sanctioned to author, is highly acknowledged. The author is highly grateful to Dr. Rajesh Sharma for providing fluid inclusion facilities at the Wadia Institute of Himalayan Geology, Dehradun.

Author Credit Statement

All the aspects of paper from conceptualization, data curation, to manuscript preparation carried out by the author.

Data Availability

Data can be made available on reasonable request from the corresponding author.

Compliance with Ethical Standards

All procedures performed in studies are as per ethical standards of the institutional and national norm. We adhere to the copyright norms.

REFERENCES

Acharyya, S.K. and Roy, A., 2000. Tectonothermal history of the Central Indian Tectonic Zone and reactivation of major faults/shear zones. J. Geol. Soc. India, 55, 239–256.

Asthana, D., Harshvardhan, K., Balakrishnan, S. and Min Feng, X., 2016. An early cretaceous analog of the 2.5 Ga Malanjkhand porphyry Cu deposit, Central India. Ore Geol. Rev., 72, 1197-1212.

Beane, R.E. and Titley, S.R., 1981, Porphyry copper deposits - Part II. Hydrothermal alteration and mineralization, in Skinner, B.J., ed., Economic Geology Seventy-Fifth Anniversary Volume, 1905-1980: El Paso, Tex., Economic Geology Publishing Co., 235-269

Bhargava, M. and Pal, A. B., 2000. Cu–Mo–Au metallogeny associated with Proterozoic tectono-magmatism in Malanjkhand porphyry copper district, Madhya Pradesh. J. Geol. Soc. India, 56, 395–413.

Bhowmik, S. K., Pal, T., Roy, A. and Pant, N. C., 1999. Evidence for Pre-Grenvillian high-pressure granulite metamorphism from the northern margin of the Sausar mobile belt in Central India. J. Geol. Soc. India, 53, 385–399.

Bhowmik, S. K., Pal, T., Roy, A., Pant, N. C. and Shome, S., 2000. Implication of Ramakona cordierite gneiss in the crustal evolution of Sausar mobile belt in Central India. Proc. Int. Seminar on Precambrian crust in Eastern and Central India, UNESCO-IUGS-IGCP-368: Geological Survey of India, Special Publication, 57, 131–150.

Bodnar, R.J., 1993. Revised equation and table for determining the freezing point depression of H_2O–NaCl solutions. Geochim. Cosmochim. Acta, 57, 683–684.

Brown, P. E., 1989. FLINCOR: a microcomputer program for the reduction and investigation of fluid inclusion data. Am. Mineralogist, 79, 1390–1393.

Chalapathi Rao, N. V., Lehmann, B., Mainkar, D. and Belyatsky, B., 2011. Petrogenesis of the end-Cretaceous diamondiferous Behradih orangeite pipe: implication for mantle plume–lithosphere interaction in the Bastar craton, Central India. Contrib. Mineral. Petrol., 161, 721–742.

Crawford, M.L., 1981. Phase equilibria in aqueous fluid inclusions. In Fluid Inclusions: Applications to Petrology (L.S. Hollister & M.L. Crawford, eds.). Mineral. Assoc. Can., Short Course Handbook 6, 75-100

Hall, D.L., Sterner, S.M. and Bodnar, R.J., 1988. Freezing point depression of NaCl–KCl–H_2O solutions. Economic Geol., 83, 197–202.

Haynes, F.M. and Kesler, S.E., 1987. Fluid inclusion chemistry in the exploration for Mississippi Valley-type deposits: an example from East Tennessee. Appl. Geochem., 2, 321–327.

Jaireth, S. and Sharma, M., 1986. Physico-chemical conditions of ore deposition in Malanjkhand copper sulphide deposit. Proc. Ind. Acad. Sci. (Earth Planet Sci), 95, 209-221.

Klemm, L.M., Pettke, T. and Heinrich, C.A., 2008. Fluid and source magma evolution of the Questa porphyry Mo deposit, New Mexico, USA. Miner. Deposita, 43, 533–552.

Kumar, S. and Rino, V., 2006. Mineralogy and geochemistry of microgranular enclaves in Palaeoproterozoic Malanjkhand granitoids, central India: evidence of magma mixing, mingling, and chemical equilibration. Contrib. Mineral. Petrol., 152, 591–609.

Kumar, S. and Rino, V., 2007. Redox series evaluation of Cu (±Mo±Au) hosting Palaeoproterozoic Malanjkhand granitoid and enclaves, Central India; evidence from magnetic susceptibility, phase petrology and geochemistry. J. Econ. Geol. Res. Manag., 4, 105-127.

Kumar, S., Rino, V. and Pal, A.B., 2004a. Field evidence of magmamixing from microgranular enclaves hosted in Palaeoproterozoic Malanjkhand granitoids, central India. Gondwana Res., 7, 539–548

Kumar, S., Rino, V. and Pal, A.B., 2004b. Typology and geochemistry of microgranular enclaves hosted in Malanjkhand granitoids, Central India. J. Geol. Soc. India, 64, 277-292.

Mollai, H., Sharma, R. and Pe-Piper, G., 2009. Copper mineralization around the Ahar batholith, north of Ahar (NW Iran): Evidence for fluid evolution and the origin of the skarn ore deposit. Ore Geol. Rev., 35, 401–414.

Naqvi, S. M., 2005. Geology and Evolution of the Indian Plate (from Hadean to Holocene 4 Ga to 4 Ka). Capital Publishing, New Delhi, 450.

Noronha, F., Dosia, A., Dubessy, J. and Charoy, B., 1992. Characterization and timing of the different types of fluids present in the barren and ore veins of the W–Sn deposit of Panasqueira, Central Portugal. Mineralium Deposita, 27, 72–79.

Pal, A. B. and Bhargava, M., 1998. Regional geology and petrochemistry of Proterozoic Cu-Mo mineralization in Malanjkhand granitoids, Madhya Pradesh. In: The Ind. Precamb., B. S. Paliwal, (Eds), Scientific Publ. (India), Jodhpur, 333-350.

Panigrahi, M.K. and Mookharjee, A., 1997. The Malanjkhand copper (±Mo) deposit, India: Mineralization from a low temperature ore-fluid of granitoid affilation. Mineral. Deposit., 32, 133-148.

Panigrahi, M. K., Naik, R. K., Pandit, D. and Misra, K. C., 2008. Reconstructing physico-chemical parameters of hydrothermal mineralization at the Malanjkhand copper deposit, India from mineral chemistry of biotite, chlorite and epidote. Geochem. J., 42, 443-460.

Rai, K.L. and Venkatesh, A.S., 1993. Geological setting and nature of copper and molybdenum mineralization in the intra-continental acid magmatic regime of Malanjkhand, central India. Resource Geology Special Issue, 15, 285–297.

Rajesh, H. M., Mukhopadhyay, J., Beukes, N. J., Gutzmer, J., Belyanin, G. A. and Armstrong, R. A., 2009. Evidence for an early Archaean granite from Bastar craton, India. J. Geol. Soc. London, 166, 193–196.

Ramachandra, H.M. and Roy, A., 1998. Geology of intrusive granitoids with particular reference to Dongargarh granite and their tectonic evolution of the Precambrian in Central India. Indian Minerals, 52, 15-32.

Richards, J.P. and Mumin, A.H., 2013. Magmatic-hydrothermal processes within an evolving Earth: Ironoxide-copper-gold and porphyry Cu ± Mo ± Au deposits. Geology, 41, 767-770.

Roedder, E., 1984. Fluid inclusions. Rev. in Mineralogy, 12, 644.

Sarkar, S.C., Kabiraj, S., Bhattacharya, S. and Pal, A.B., 1996. Nature, origin and evolution of the granitoid-hosted early Proterozoic copper–molybdenum mineralization at Malanjkhand, central India. Mineralium Deposita, 31, 419–431.

Seo, J.H., Guillong, M. and Heinrich, C.A., 2009. The role of sulphur in the formation of magmatic-hydrothermal copper–gold deposits. Earth Planet. Sci. Lett., 282, 323–328.

Sikka, D.B. and Nehru, C.E., 1997. Review of Precambrian porphyry Cu±Mo±Au deposits with special reference to Malanjkhand porphyry copper deposits, M.P.J. Geol. SOC. review of recent ideas on their origin. Proc. Int. Symp. on ‘Geol. of granites and their metallogenetic relations’. Nanjing Uni, Nanjing, China., 137-144.

Srivastava, R.K. and Gautam, G.C., 2009. Precambrian mafic magmatism in the Bastar craton, central India. J. Geol. Soc. India, 73, 52–72

Srivastava, R. K., Chalapathi Rao, N. V. and Sinha, A. K., 2009. Cretaceous potassic intrusives with affinities to aillikites from Jharia area: Magmatic expression of metasomatically veined and thinned lithospheric mantle beneath Singhbhum craton, Eastern India. Lithos, 112, 407–418.

Stein, H.J., Hannah, J.L., Zimmerman, A., Markey, R.J., Sarkar, S.C. and Pal, A.B., 2004. A 2.5 Ga porphyry Cu-Mo-Au deposit at Malanjkhand, central India: implications for Late Archean continental assembly. Precamb. Res., 134, 189–226.

Tripathi, C., 1979. The Malanjkhand-Taregaon porphyry Cu deposits. Geol. Surv. India, Misc. Publ., 34, 161-168.

Zhang, Y.G. and Frantz, J.D., 1989. Experimental determination of the compositional limits of immiscibility in the system $CaCl_2$–H_2O–CO_2 at high temperatures and pressures using synthetic fluid inclusions. Chem. Geol., 74, 289–308.

Received on: 31-07-2024 ; Revised on: 06-11-2024; Accepted on: 06-11-2024